Optimization of AlN materials on special uses

Axel Kranzmann, Günter Petzow
Max-Planck-Institut für Metallforschung
Pulvermetallurgisches Laboratorium
Stuttgart, FRG

The sintering behaviour of AlN powders doped with different oxides such as MgO, CaO, Al_2O_3, Y_2O_3 and La_2O_3 were investigated. Mechanical and thermal properties such as bending strength, thermal expansion and heat conductivity were experimentally estimated. Depending on the phase composition a wide range of property values were observed.
The last two decades of investigations on AlN mainly stress the aspect of high thermal conductivity and the ultimate goal of most of the work was an AlN substrate material with high thermal conductivity. The mechanisms limiting heat conductivity by enhanced phonon scattering and the sources of these mechanisms will be described. Quantitative calculations of heat conductivity for several compositions substantiate the idea that impurity atoms reduce the heat conductivity of the AlN grain. The role of microstructure can be discussed qualitatively coupling the internal contact area of a polycrystal material with the grain to grain heat transition First ideas of a microstructure description which did not approach the grain as an ellipsoid were developed. On the base of that knowledge AlN ceramic with more than 200 $W \cdot m^{-1} \cdot K^{-1}$ heat conductivity and gradient materials with high surface oxidation resistance were developed.
The heat conductivity is influenced by the impurities dissolved in the AlN grains and the formation of grain contact area, which depends on the grain form, whereas the mechanical strength of the AlN materials is strongly correlated to the grain size.
The greatest benefit in establishing AlN ceramics would be to develop a material with improved mechanical strength and high oxidation resistance without loss of high thermal conduction. Uses in microwave technology could be possible for high heat conducting high strength AlN. It is expected that fine AlN powders doped with Y_2O_3 or CaO sintered to ceramics with less than 3 μm medium grain size will exhibit more than 400 MPa bending strength and thermal conductivity values of about 150 $W \cdot m^{-1} \cdot K^{-1}$. Forming a chemical gradient of the oxygen content of less than 100 μm thickness at the surface region results in additional high oxidation resistance.

I) Introduction

III-V compounds are widely investigated on their use as semiconductor materials /LAB82, LAB84/. The compounds between the elements of the III and V group of the periodic system mainly crystallize in the zinc-blende, diamond or wurtzite structure, which are all very similar to the diamond lattice symmetry. In the cubic binary III-V composites group III atoms occupy all on one of the possible fcc sub-lattice while the group V atoms lie on the other /OLE78/. The Nitride III-V compounds such as BN, AlN crystallize in the hexagonal symmetry of the wurtzite type, with two AlN units per unit cell. The space group 6_3mc describes the symmetry of the wurtzite structure and the lattice constants are found to be $a = (311.1 \pm 0.1)$ pm and $c = (498.0 \pm 0.1)$ pm /TAY60/. The lattice symmetry, the low number of atoms per unit cell, the mass differences between the atoms in the unit cell and the binding forces determine the heat conductivity of the pure crystal /STP87, KRA88/. The similarity of the wurtzite structure to the diamond structure, the material with the highest phonon thermal conductivity, is the reason for the good thermal conductivity of cubic and hexagonal III-V compounds. With the phonon model it is possible to calculate the thermal conductivity of simple crystal structures, such as AlN, and the influence of point defects /RKP90/. To design AlN ceramics the ultimate goal of our studies was to develop the knowledge about material preparation as well as it is necessary for the sintering of suitable materials in different uses.

II) Sample preparation

II.1 powder processing

All samples were prepared from AlN grade A, H.C. Starck, Berlin. The AlN powder and the sinter additives were mixed using an attrition mill with 500 ml volume. One charge contained 100 g AlN powder, the sinter aid and 200 ml isopropanol. Table 1 summarize the powder compositions used in this work. The milling tools, balls and attrition arm, consists of Al_2O_3. The rubbed material from the tools and the water content of the isopropanol increased the oxygen content of the powder up to 3.5 wt.%, fig. 1. Other impurities found by TEM-EDX analysis in the sintered state are Mg, Si, La, Zr, Fe and Cr /SOC90/. Whereas Fe and Cr are also found in the original AlN powder and La in the original Y_2O_3 powder, the source for Mg and Si is rubbed material from the milling apparatus. The origin of Zr was not identified. During milling the specific surface area and the oxygen content of the powder increased, fig. 1. Because it is expected that all additional oxygen picked up during milling procedure is concentrated in an $Al(OH)_3$ layer at the particle surface, the oxygen can be trapped in the liquid face formed during sintering

Sample	Additive	Additive portion [wt.%]	BET surface [$m^2 \cdot g^{-1}$]	impurity content [wt.%]
AM	MgO	1	10.9	O (4.7)
AC1	CaO	1	8.5	O (3.5)
AC14	CaO	1.4	8.2	O (3.5);Si (0.16)
AC2	CaO	2	8.3	O (3.8)
ACS0	$CaO \cdot SiO_2$	0.6	7.1	O (0.27)
ACS1	$CaO \cdot SiO_2$	1.3	7.5	O (3.0)
ACS2	$CaO \cdot SiO_2$	2.5	7.6	O (3.5)
AA	Al_2O_3	2.5	9.1	O (5.6)
AL	$1La_2O_3 \cdot 6Al_2O_3$	2.3/4.5	6.1	O (4.5)
AY	Y_2O_3/C	2.5/1	5.9	O (2.5)

Tab. 1: Powder specifications for the different AlN materials after milling.

process. After fast drying at 370 K, Rotavapor, the powders were sieved, encapsulated in rubber forms and hydrostatically pressed at a pressure of 630 MPa. The green density was always between 59 and 62 % of the theoretical density of the powder mixture.

II.2 Sintering and Annealing

The consolidated green products were sintered in a graphite heated sinter furnace in N_2 atmosphere at 10^5 Pa pressure. In the same furnace additional heat treatments on samples of the composition AC14 were carried out at sintering temperature. Partially these heat treatments were done with a powder bed consisting of 80 wt.% AlN and 20 wt% carbon black to enforce evaporation of oxygen from the grain boundaries of the material. During the annealing procedure the samples lost oxygen and after that the Ca was evaporated /RUC89/. The grain boundary phase evaporation in contact with a powder bed (80wt% AlN, 20wt% CaO) for CaO doped samples give very similar results to the experiments on AlN/Y_2O_3 materials /UEH89/. After 24h the oxygen and the calcium content reached the lowest levels below 0.3 and 0.1 mass%, respectively. Further annealing gave no further change of the level of dissolved O and Ca but a reduction of the total impurity level was still observable and subsequently the heat conductivity increased from < 100 to 219 $W \cdot m^{-1} \cdot K^{-1}$. Dissolved Si in AlN grains analysed during TEM observation by an EDX-analyzer was correlated with the existence of line faults which are assumed to be anti phase boundaries /RUC89/. The observed line defects were always connected

with Ca inclusions in the AlN crystal. The dissolution of Ca at sintering temperatures and the segregation of Ca during cooling period could be one explanation of this observation. The line defects and the Si atoms act as phonon scatterers producing low heat conductivity increase during the first 24 h annealing time, fig. 2.

A second way to eliminate grain boundary phase was experimentally developed on Y_2O_3 doped AlN powders. Volumes of $40 \cdot 25 \cdot 5$ mm^3 AlN material (AY) were pressed in an Al_2O_3 powder bed and annealed in laboratory atmosphere at 1120 and 1220 K, respectively. During the treatment the carbon and the Y content decreased and the heat conductivity increased from 80 to 149 $W \cdot m^{-1} \cdot K^{-1}$. In a small surface region of less than 100 μm thickness an increase of Oxygen was observed by WDX analysis, fig. 3.

It is suggested that the driving force for the observed grain boundary modifications in reducing atmosphere or in a powder bed is the chemical gradient. In reducing atmosphere the evaporation process depends on the total pressure of CO_2 and CO and if the nitration of reduced Al_2O_3 occurs also on the N_2 pressure/UMK90/. Therefore the reducing effect of the atmosphere is modulated by temperature and pressure.

In a powder bed containing Al_2O_3 which is also present in the microstructure an equal distribution of Y_2O_3 should form. The Y_2O_3 diffuses in the powder bed, the C reduces the oxygen content in the grain boundary so that in result no oxidation of the whole bulk was observed. The partial oxidation of the surface results in a AlN material with oxidation resistant surface.

Sample	Identified phases + AlN	sinter temperature [K]	heating rate [K·min^{-1}]	sinter time [min]
AM	$MgAl_2O_4$	2220	20	5
AC1	$CaAl_4O_7$	2090	15	15
AC14	$CaAl_4O_7$	2095	15	15
AC2	$CaAl_4O_7$	2090	15	30
ASC0	2Hδ $\equiv Si_{2.4}Al_{8.6}O_{0.6}N_{11.4}$	2120	15	15
ASC1	2Hδ	2120	15	15
ASC2	2Hδ, $CaAl_2O_7$	2120	18	15
AA	27R Polytype $\equiv Al_9O_3N_7$	2270	33	15
AL	$LaAlO_3$, $\beta-Al_2O_3$	2120	12	5
AY	$Y_3Al_5O_{12}$	2220	20	20

Tab. 2: Sinter conditions and phases detected by X-RAY analysis.

III) Material testing and characterization procedures

III.1 Mechanical Testing

For bending strength test bars with dimension of $4.5 \cdot 3.5 \cdot 55$ mm^3 were cut. One surface, $3.5 \cdot 55$ mm^2, was polished to mean roughness smaller than 0.1 μm. The roughness was estimated by an optical surface roughness testing assembly, Rodenstock RM400. All samples were tested in 4 point bending test, 40/20 mm support, with a spindle velocity of 0.1 mm$\cdot$min^{-1}. Comparisons with experiments using hydropneumatic equipment exhibit no different results. Therefore low velocity crack propagation can be neglected.

III.2 Thermal Conductivity Measurements

Two different methods were used for thermal conductivity measurements. A direct measurement of the temperature field in a steady state assembly /KRA88/ and laser flash method /PJB61/, Conductronic, Theta industries. The direct method used here is restricted in temperature range. Experiments in the temperature range between 250 and 500 K are possible. The laser flash equipment operates from 400 to 2000 K. The heater of the direct method is easily controlled by a computer assembly. The heat source of the pulse method is a light pulse irradiated from a NdY-Garnet laser system. The run time of the heat pulse is measured by an InSb detector whose signal is recorded by a storage oscilloscope. For the steady state equipment the sample size is $35 \cdot 8.5 \cdot 8.5$ mm^3, which is a 5 times larger volume than the cylinders of 10 mm diameter and 5 mm thickness investigated in a laser flash experiment. The probability that inhomogeneities such as small cracks or porosity bands will be influencing the material property proportional to the sample size. Additionally the transparency of very pure AlN can suggest a higher thermal conductivity in laser flash experiments. Covering the surface with a C or Cr layer is only a protection against the transmittance of laser light intensity. But still the irradiated surface can be seen by the detector because of the grey radiation of any volume element of the material. At higher temperatures the transmission coefficient is small and successful laser experiments were carried out.

III.3 Microstructure characterization

The microstructure of the samples was characterized in terms of stereometric and fractal description. The difference in solubility and mobility of Al and N atoms dissolved in the glassy phase results in differences in the mean of the maximum Ferets diameter per grain. The biggest grains in this term were observed in the AY material, 7.0 ± 1.8 μm.
The smallest AlN grains exhibit the AlN - 27R composite ceramic, 1.8 ± 0.7 μm. In all

materials the mean ratio between longest and shortest dimension of the AlN grains in a plane polished surface was estimated to be 1.4 ± 0.4. This indicates that all grains are slightly elongated. This simple form of microstructure characterization includes no information about the grain to grain heat transfer, because this kind of description is an elliptical approximation. But ellipsoids forms only point like contacts between each other. In a real AlN microstructure all varieties of grain contacts between point contacts and surface to surface contacts will be formed during sintering, fig. 4. In annealed samples with high thermal conductivity the grains exhibit more or less plane surface contacts between each other. The change from globular to polyhedral grains can be easily described in terms of topology and fractal geometry.

A microstructure consisting of only globular and dense packed grains and zero porosity the number of crystalline plane faces of each grain is zero and the number of next neighbours is twelve but the contact area is zero. If all grains are polyhedrons and dense packed, the number of plane faces and next neighbours are equal and the plane interface area is equal to one half of the total internal surface. It is expected that curved interface will result in an enhanced phonon scattering /RKP90/, plane interfaces are more effective in heat transfer from grain to grain.

Basing on topological and fractal geometry parameters a microstructure description was developed which contains information about the form of grain to grain contact. The so called planarity of the microstructure was defined as,

$$P_l := \frac{N_C \cdot D_t}{N_N \cdot D_f}$$

, where the number of corners, N_C, and next neighbours, N_N, per grain is connected with the fractal dimension, D_f, of a path along the grain boundaries and the corresponding topological Dimension, D_t, which is 1 for a path along grain boundaries in a plane section such as mostly investigated by material scientists /RUC89/. In good agreement with the explained model an increasing planarity results in an increasing thermal conductivity, fig. 5. After sintering the fractal dimension of path along the grain boundary lines is in the range of 1.15 and already very close to the expected dimension 1 for the exact polygons of the grain outlines in the plane section if all grains were polyhedrons.

The mean free path length of phonons in the AlN grain is smaller than 10^{-8} m and therefore no relation between grain size and thermal conductivity is expected as long as the grains are bigger than the mean free path length. This consideration is demonstrated by the observation of the thermal conductivity of materials with different grain size, fig. 6.

IV) Optimized AlN materials

IV.1 Mechanical strength

The mechanical strength of AlN varies not remarkably with the kind of additive /RKP90/, but changes slightly with the grain size. The investigation of the effect on the mechanical strength demonstrated that the defect size is joint with the grain size, fig 7. Small grains, mean diameter smaller than 3 μm, are necessary for high mechanical strength. Two AlN materials compositions were found which can be densified without accelerated grain growth, AC and AL. The investigation of the AC materials show that the densification depends on the volume fraction of sinter additive. As observed in several Alkaline earth doped AlN qualities, high amounts of additives produce porous samples the limiting fractions were estimated to be MgO $\geq$ 2, CaO $\geq$ 2.5 and BaO $\geq$3 wt%.
Therefore the investigation of various amounts of CaO additive is limited to a small range.
La_2O_3 doped AlN sinters to full density independent of the amount of additive. The mechanical strength and fracture modulus varied with the ratio between La_2O_3/Al_2O_3, which is again connected with the grain size, fig. 8, /BKP89/.

IV.2 Dielectric strength

The dielectric strength of AlN substrates is not understood in a way which enables to modulate the dielectric breakdown voltage. Several mechanisms can be responsible for the breakdown. At high frequencies dielectric coupling of the material is possible. A heat induced breakdown through the glassy phase can be possible. Based on the observation that some pA current flowed at DC-voltages of more than 1 kV across 0.5 mm demonstrates that also under a direct voltage test a self heating and a subsequent breakdown is possible. The polarization breakdown seems to be more unlikely and should only be observed under direct voltage testing of very pure AlN ceramic /RKP89/. If inclusions with a different polarizability exist in the microstructure the dielectric breakdown voltage will decrease. In computer simulation the breakdown path connects the actual breakdown tip with the next inclusion /KOL90/.

IV.3 Thermal conductivity

The different AlN materials exhibit strong differences in heat conductivity, tab. 3. The maximum heat conductivity of a heterogeneous two phase AlN material was observed on CaO doped AlN ceramic. That is a slightly higher thermal conductivity than observed on hot pressed CaO doped AlN and comparable with hot pressed Y_2O_3 doped AlN

Dopant in wt%	Distribution and shape of second phases	λ $W \cdot m^{-1} \cdot K^{-1}$	$d\lambda/dt$ $W \cdot m^{-1} \cdot K^{-2}$
AA	D;c/a ≃ 5; d_{max} ≃ 10 μm	60 ± 3	≃ 0
ACS0	TP (Glass) and the SiAlON	48 ± 2	- 0.01
ACS1	c/a ≃ 11; d_{max} ≃ 8 μm	46 ± 1	- 0.01
ACS2		35 ± 1	< - 0.01
AM	TP	117 ± 6	- 0.07
AC1	TP	148 ± 7	- 0.11
AC14	TP (as sintered)	48 ± 21	< - 0.1
AC14	single phase, annealed	219 ± 37	- 0.6
AY	TP	81 ± 4	- 0.08
AL	TP	84 ± 4	——

TP - Tripel point
D - Second phase is disperse with the maximal particle size d_{max} and the medium aspect ratio c/a.

Table 3: Heat conductivity and the first derivative of the heat conductivity with respect to the temperature.

/KUT88/. Due to the formation of the 27R-polytype and the saturation of the AlN grains with O, undoped AlN materials with oxygen contents higher or equal than 3,5 wt% has a heat conductivity which is always lower than 75 $W \cdot m^{-1} \cdot K^{-1}$.
Oxygen contents between 3,4 wt% and 15 wt% do not change the lattice parameters of AlN indicating a constant lattice oxygen content /KRA88,SLA73/. The formation of a second phase, table 2, and the dissolving of other impurity atoms like Si or C can also be reasons for decreasing the heat conductivity of the material. The influence on heat conductivity from impurity scattering of lattice phonons is much more important than the influence of the distribution and the kind of second phase.
The x-ray data from the AlN lattice constants indicate that, in all the considered types of AlN ceramic, a residual lattice distortion exists. This observation can be a result of the presence of point and/or line defects as observed in AlN materials. Both will decrease the heat conductivity of the material /ABE63, ZIM79/.
The derivative of the heat conductivity λ with respect to the temperature T indicates

the perfection of the AlN lattice /KRA88/ and is an indication of the phonon scattering mechanisms /ZIM79/. High point defect densities in AlN such as impurity atoms and vacancies result in a temperature derivative $\nabla_T \lambda /_{T=300\ K}$ between -0.04 and -0.1 $W \cdot m^{-1} \cdot K^{-2}$. Very pure AlN materials should exhibit a temperature dependence similar to that of to AlN single crystals where $\nabla_T \lambda /_{T=300\ K} = -1.7\ W \cdot m^{-1} \cdot K^{-2}$ is experimental estimated /SLA73/, which is in confirmation with the calculated value /KRA88/.
If the quantity of the impurity atoms dissolved in the AlN lattice and the distribution, the heat conductivity and the volume content of the second phase are known a calculation of the heat conductivity can be made. In the case of oxygen as the single impurity with an assumed maximum solubility of 1.6 wt% in the AlN lattice /SLA73/ and a content of 16,2 vol% 27R-AlN-polytype with a heat conductivity of 6,3 $W \cdot m^{-1} \cdot K^{-1}$ /SAK78/, the calculated heat conductivity and the measured values are within a range of 8% /KRA89/. The content of 27R-polytype is calculated with the assumption that all oxygen not dissolved in the lattice goes to form the polytype.
The results of model calculations demonstrate, that dissolved impurities are strongly decreasing the thermal conductivity. An optimal heat conducting AlN ceramic has a microstructure such as in fig. 9 and a very low impurity content. All scientists who anneal their samples found increasing thermal conductivity with decreasing impurity content. If impurity content decreases and grain growth occurs, microstructural and chemical effect add each other. The grain diameter is negligible as long as it is no limitation for phonon transport. The free path of phonons in AlN estimated from simple Debye formula,

$$l_{Ph} = 3 \cdot \frac{\lambda}{v \cdot C}$$

,where the thermal conductivity, λ, the heat capacity, C, and die sound velocity, v, can

impurity atom	fraction wt %	thermal conductivity, λ $W \cdot m^{-1} \cdot K^{-1}$	$\frac{d\lambda}{dT}$ / $W \cdot m^{-1} \cdot K^{-2}$
Si	0.12	185	- 0.5
Mg	0.11	80	- 0.05
	0.05	115	- 0.16
O+C	3.41 + 2.56	59	$\cong$ 0
Al_2OC	1.71 + 1.28	87	- 0.07

Table 4: Calculated heat conductivities and calculated temperature derivation of the heat conductivity at 300 K in dependence on different impurities.

be used to calculate the mean free path length, l_{Ph}, of the phonons, is smaller than $4.7 \cdot 10^{-8}$ m (λ = 320 $W \cdot m^{-1} \cdot K^{-1}$, C = $2.54 \cdot 10^6$ $J \cdot m^{-3} \cdot K^{-1}$, $\bar{v}$ = 8000 $m \cdot s^{-1}$).

IV.4 Gradient material with improved oxidation resistance

The oxidation resistance of AlN – $Al_9O_3N_7$ composite material was used to form a oxidation resistant layer on a high thermal conducting AlN material, fig. 10. The material was prepared by infiltration of the green product of composition AC14 with water. According to the reaction,

$$AlN(s) + H_2O(l) \Longrightarrow Al(OH)_3(s) + NH_3(g)$$

, an Aluminiumhydroxide forms on the AlN surface. The excess heat from this exothermic reaction has to be removed from the sample or it will be destroyed by the vapour pressure of boiling water.

After sintering procedure, equal to the samples AC14, tab. 2, a material with a continuous change in microstructure and oxygen content is formed. With the oxygen content the coexisting phases vary and the properties are modulated by this variation. Three characteristic microstructures intermesh continuously. The volume in direct contact with the water bath consists of elongated 27R grains, mean length $\cong$ 25 μm, AlN, $CaAl_{12}O_{19}$, AlN and a glassy phase. This phase assembly changes to AlN, $CaAl_{12}O_{19}$ and glass after 1 cm infiltration depth. After 2 cm thickness the normal AC14 microstructure was observed. The total length of the cylindric sample was 8 cm and 50 ml water was used for infiltration. The diameter of the sample amount to 2.5 cm. The infiltration depth can be controlled by infiltration time and/or total water quantity. Compared with a subsequent treatment such as annealing in an Al_2O_3 powder bed as described above, the infiltration with water is fast and inexpensive but the penetration depth is more difficult to control. The pressing of samples with layers of different powder qualities will produce a differential shrinkage during sintering because of different grain size distribution, fig 10. The local properties of the developed AlN-gradient material are represented in fig. 11. AlN materials such as the developed one can be used as heat exchangers in oxidizing atmosphere, heat lines or heating elements with partially isolating surface can be constructed.

V) Summary and Conclusions

AlN material with high transparency and high thermal conductivity used in optical applications will exhibit a grain size bigger than 5 μm. Such material cannot be applied in uses where strength values of more than 400 MPa are necessary such as microwave window for a high energy microwave system. AlN heat exchangers in oxidizing atmospheres will be destroyed by rapid oxidation, if the surface is not protected. By infiltration of the green product surface with water such a protection is developed. The use of the material at temperatures less than 1300 K in an oxidizing environment is possible. The bulk material is still high thermal conducting AlN. A similar effect can be produced if the material is in contact with Al_2O_3 during annealing time in normal atmosphere but at temperatures lower than 1170 K. The last procedure offers the benefit, that lower annealing temperatures and simpler furnace system can be applied.

High strength AlN can be produced, if during consolidation the grains remain below 3 μm mean grain size. The thermal conductivity will not be reduced if the grains are formed like polyhedrons. The base for such a development is AlN powder with a grain size small enough, that grain growth with a simultaneous forming of facets is possible during sintering without passing over the 3 μm limitation for grain size.

Literature

/ABE64/ B. Abeles, Phys. Rev. 5, 131 (1964) 1906

/BKP89/ J.-P. Bazin, A. Kranzmann, G. Petzow, Proceedings of the 1. European Ceramic Society Conference, ECERS, Maastrich, 1989, vol. 3, 419.

/KOL90/ R. Köller, MPI für Metallforschung, Institut für Werkstoffwissenschaft, PML, private communication.

/KRA88/ A. Kranzmann, PhDThesis, University Stuttgart, 1988.

/KRA89/ A. Kranzmann,S. Ruckmich, G. Petzow, Proceedings 1.Meeting of the European Material Society, FEMS 89, Aachen.

/KUT88/ Y. Kurokawa, K. Utsumi, H. Takamizawa, J. Am.Ceram. Soc. 71 (1988) 588.

/LAB82/ Landoldt-Börnstein, Neue Serie, Bd. 17a

/LAB84/ Landoldt-Börnstein, Neue Serie, Bd. 17c

/OLE78/ G.H. Olsen, M. Ettenberg, in: Crystal Growth, vol.2, ed. by C.H.L. Goodman, 1978, Plenum Press.

/PJB61/ W.J. Parker, R.J. Jenkins, C.P. Butler, G.L. Abbott, J. Applied Physics 32, 9(1961)1679.

/RKP89/ R. Köller, A. Kranzmann, G. Petzow,"The dielectric breakdown of AlN substrate materials", poster contribution to the 1.Meeting of the European Material Society, FEMS 89, Aachen.

/RKB90/ S. Ruckmich, A. Kranzmann, E. Bischoff, R.J. Brook, "The description of microstructure applied on the thermal conductivity of AlN substrate material", submitted to the J. of the European Ceramic Society.

/RKP90/ S. Ruckmich, A. Kranzmann, G. Petzow, "Properties and microstructure of pressureless sintered AlN-substrate materials", Proceedings of the 7th CIMTEC, Montecatine Therme, Italy, 1990, in press.

/RUC89/ S. Ruckmich, diploma piece, University Stuttgart, 1989.

/SAK78/ T. Sakai, Yogyo-Kyokai-Shi 3, 86 (1978) 125.
/SLA73/ G.A. Slack, J. Phys. Chem. Solids 34 (1973) 321.
/SOC90/ H. Sockel, Universität Erlangen, priv. communication.
/STP87/ G.A. Slack, R.A. Tanzili, R.O. Pohl, J.W. Vandersande, J. Phys. Chem. Solids 48, 7(1987)641.
/TAN89/ K. Tani, Niihama National College of Technology, Japan, unpublished data.
/TAY60/ K.M. Taylor, C. Lenie, J. Electrochem. Soc. 107(1960)308
/UEH89/ Fumio Ueno, Akihiro Horiguchi, Proceedings of the First European Ceramic Society Conference (ECerS'89), Maastricht, The Netherlands, Elsevier Publishers, Bd.1, 383.
/UMK90/ E. Udagawa, H. Makihara, N. Kamehara, K. Niwa, J. of Mat. Science Letters, 9(1990)116.
/ZIM79/ J.M. Ziman, "Electrons and Phonons". Oxford at the Clarendon Press, first edition 1960.

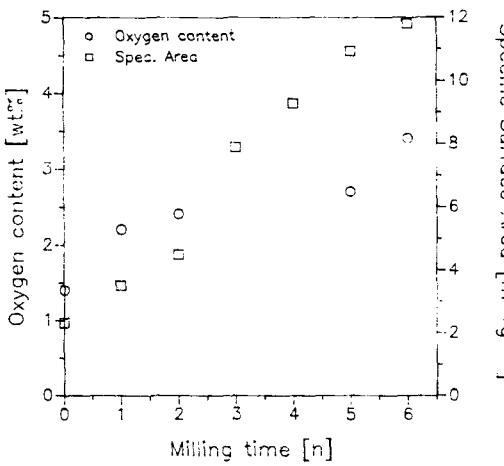

Fig. 1: The influence of the milling procedure on the oxygen content and the specific surface (BET) of the powder mixture.

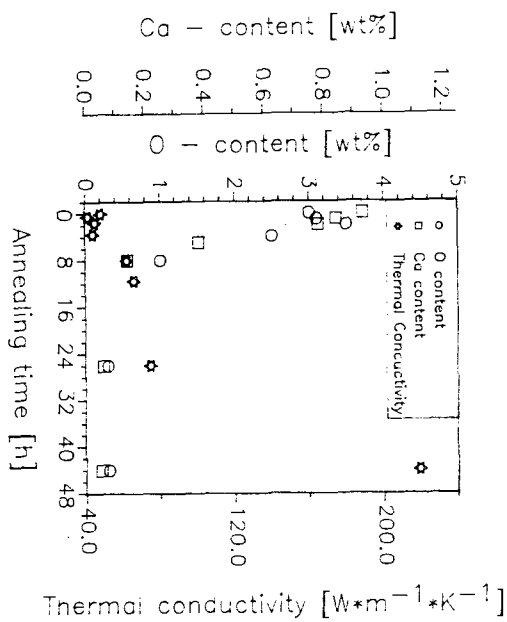

Fig. 2: Decrease of impurity level and subsequent increase of heat conductivity of the samples AC14 during annealing time.

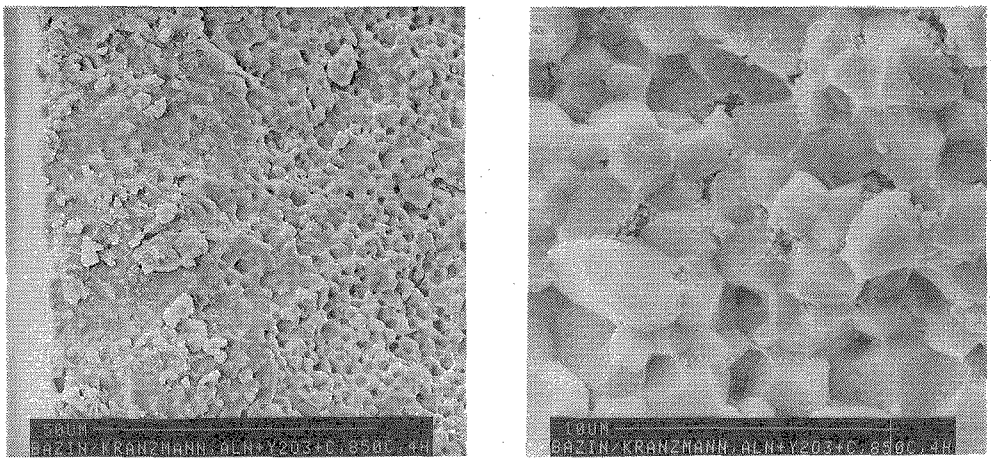

a) b)

Fig. 3: SEM micrographs of fracture surface showing the surface modification during annealing samples AY in an alumina powder bed. a)Oxidized surface layer, b) bulk material.

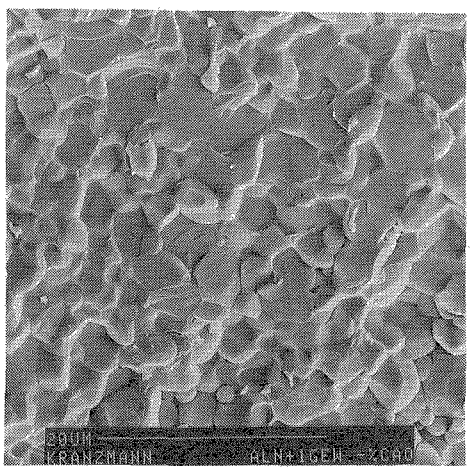

Fig. 4: SEM micrograph of fracture surface of CaO doped AlN (AC1) after sintering.

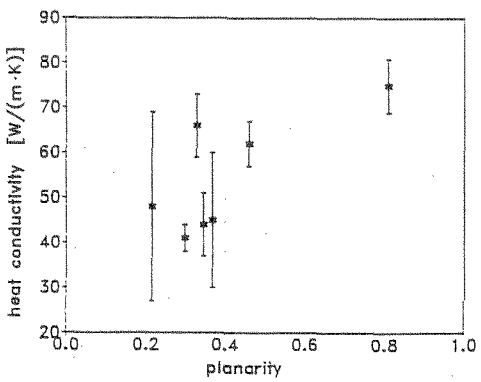

Fig. 5: Variation of heat conductivity with the planarity of the microstructure.

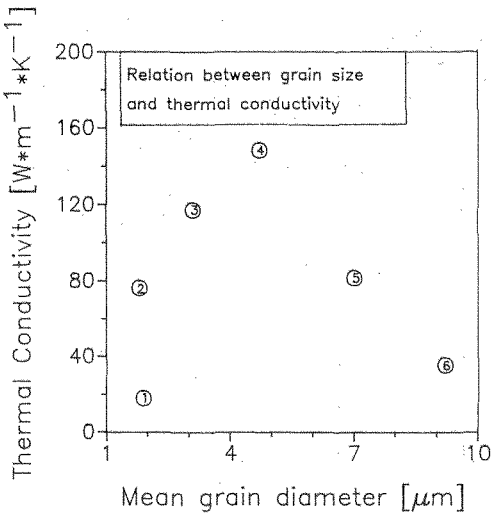

Fig. 6: Influence of grain size on the thermal conductivity of samples: 1)AlN + 10 wt% $CaO \cdot SiO_2$ /KRA88/, 2)AA, 3) AM, 4)AC1, 5)AY, 6)AlN + 5 wt% BaO /TAN89/.

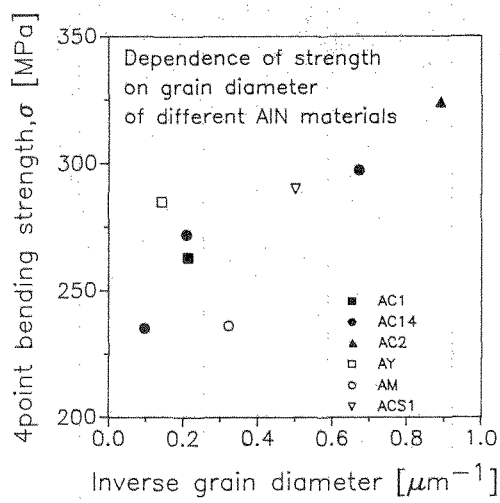

Fig. 7: Relation between grain size and bending strength of AlN materials.

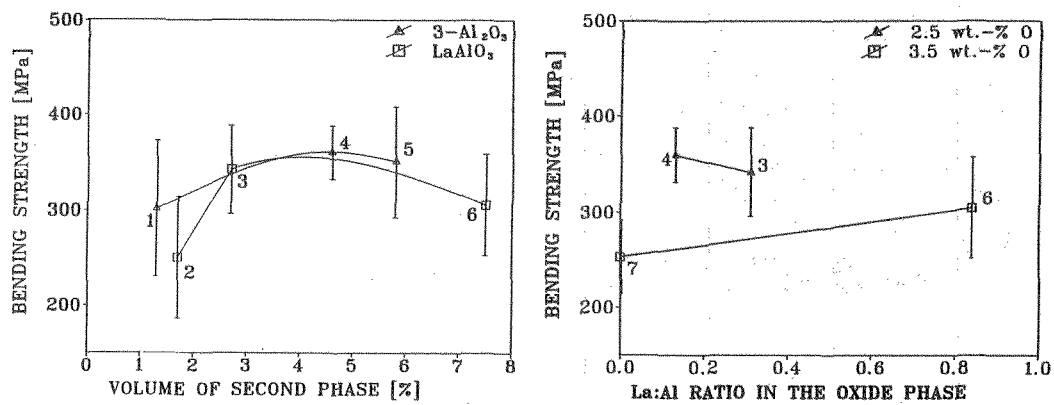

a) b)

Fig. 8: Bending strength as a function of a) the volume fraction of the second phase and b) the molar ratio La:Al.

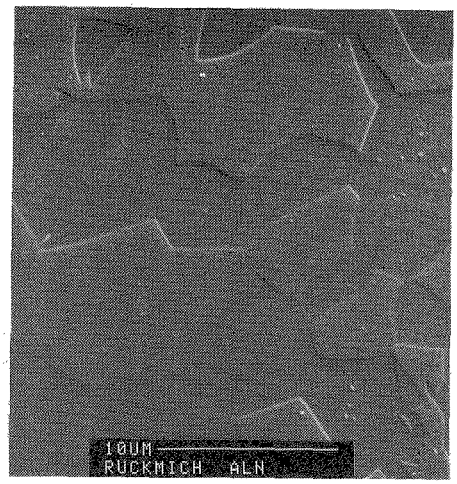

Fig. 9: SEM micrograph of high thermal conducting AlN (sample AC14, 44h annealed at T = 2120 K).

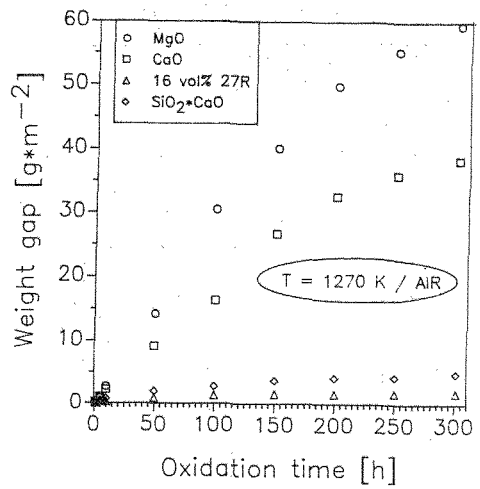

Fig. 10: Oxidation resistance of AlN doped with MgO (1 wt%), CaO (1 wt%), $CaO \cdot SiO_2$ (1.25 wt%) and AlN - 27R composite material.

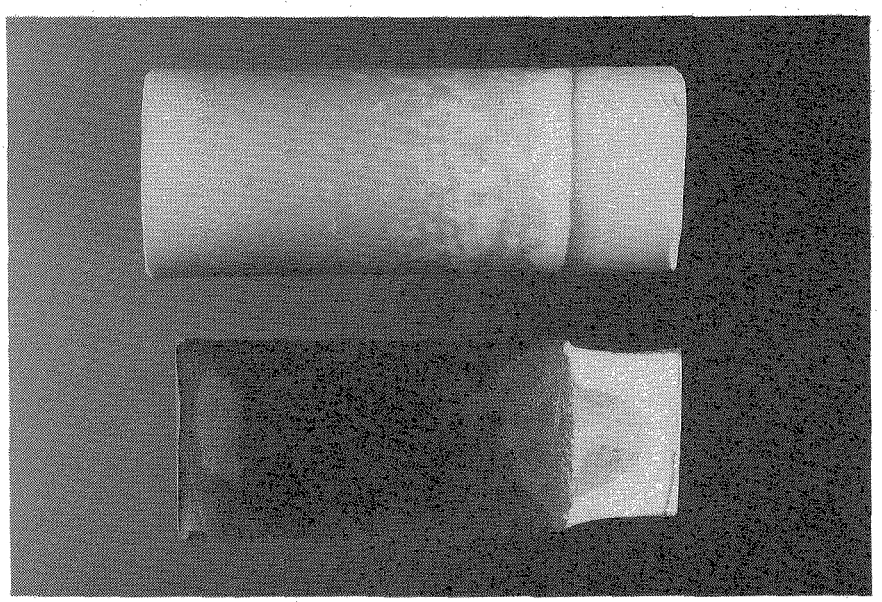

Fig. 11: Total view of two AlN-FGM samples. a) Water infiltrated AlN. The reaction frontier is observable as a dark contrast line. b) Sample sintered from a hydrostatically pressed two layer green product. The white layer is AlN, Tokuyama Soda Grade F with 1.2 wt% oxygen, and the dark layer consists of AlN, H.C. Starck Grade C with 1.8 wt% O. The difference in pressing behaviour and total shrinkage formed a inhomogeneous sample diameter

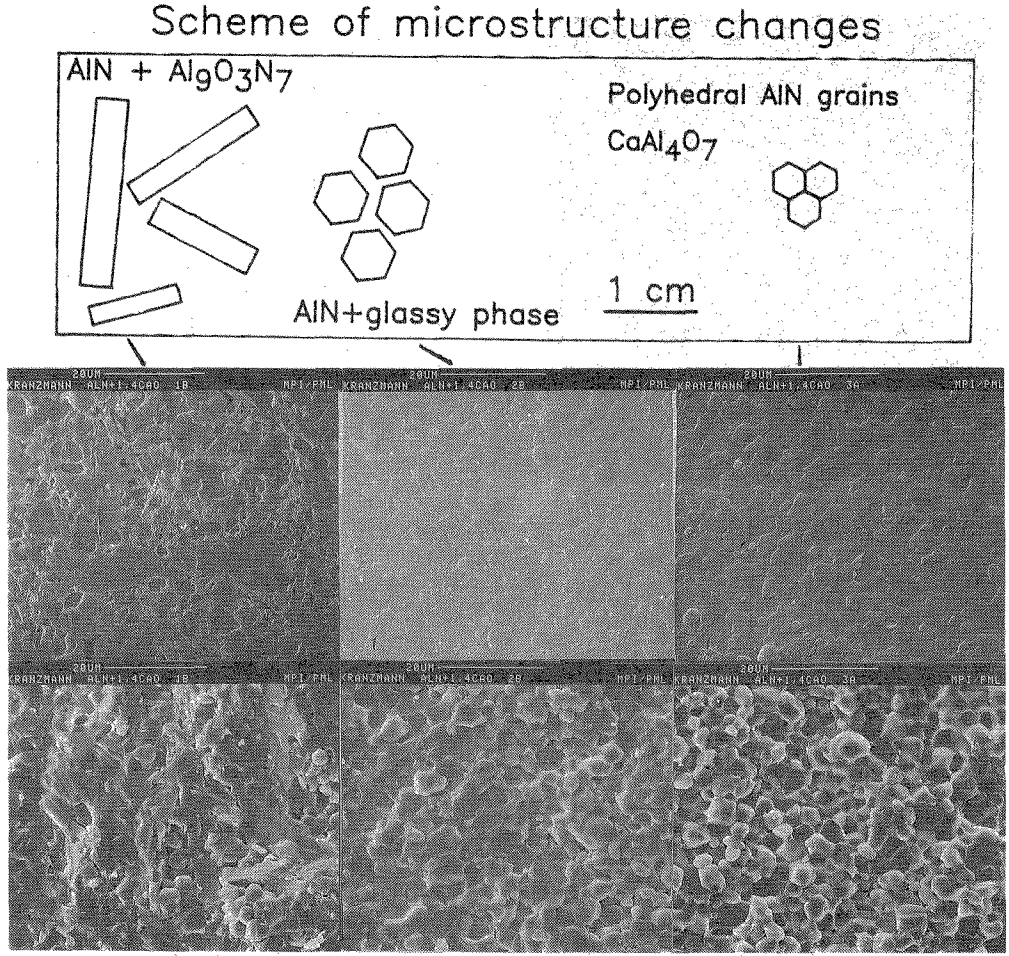

c)

Distance from surface / cm		0 - 1	≅ 1.5	> 2
ΔM	/ g·m^{-2}	1.71 ± 0.04	4.83 ± 0.04	38.26 ± 0.04
V_{27R}	/ vol%	20 ± 1	5 ± 1	0
O_C	/ wt%	5 ± 0.5	3.2 ± 0.3	3.0 ± 0.3
σ	/ MPa	280 ± 38	270 ± 25	297 ± 22
K_{IC}	/ MPa·$\sqrt{m}$	3 ± 0.2	3.1 ± 0.2	3.5 ± 0.3
λ	/W·m^{-1}·K^{-1}	45 ± 2	64 ± 0.2	148 ± 5

Fig. 12: a) Schematic Microstructure of the AlN -FGM. b) SEM micrographs of selected areas, upper series polished and lower series fracture surfaces.
c) Distribution of oxidation resistance, weight gain, ΔM, after 300 h oxidation in air, volume fraction of 27R phase, V_{27R}, total oxygen content, O_C, 4-point bending strength, σ, fracture toughness K_{IC} and thermal conductivity, λ.